Effect of long-range interaction on graphene edge magnetism

Zheng Shi* and Ian Affleck

Department of Physics and Astronomy, University of British Columbia, Vancouver, British Columbia, Canada V6T 1Z1

(Received 1 February 2017; published 19 May 2017)

It has been proposed that interactions lead to ferromagnetism on a zigzag edge of a graphene sheet. While not yet directly studied experimentally, dramatically improving techniques for making and studying clean zigzag edges may soon make this possible. So far, most theoretical investigations of this claim have been based on mean-field theories or more exact calculations using the Hubbard model. But long-range Coulomb interactions are unscreened in graphene, so it is important to consider their effects. We study rather general nonlocal interactions, including of the Coulomb $1/r$ form, using the technique of projection to a strongly interacting edge Hamiltonian, valid at first order in the interactions. The ground states as well as electron/hole and exciton excitations are studied in this model. Our results indicate that ferromagnetism survives with unscreened Coulomb interactions.

DOI: 10.1103/PhysRevB.95.195420

I. INTRODUCTION

Noninteracting graphene nanoribbons with zigzag edges are famous for hosting a nearly flat band of edge states [1,2]. In the presence of electron-electron interaction, the existence of edge magnetic order [3] has been predicted by a multitude of theoretical work using both analytical [1,4–11] and numerical [12–20] techniques. The consensus emerging from these works is that edge states localized at the same edge are coupled ferromagnetically to form superspins, which then couple antiferromagnetically between edges. In addition to ground-state properties, low-energy magnetic excitations in graphene nanoribbons have also attracted much theoretical attention [6,9,21,22]. A relatively large spin-correlation length up to the order of micrometers has been found for a single zigzag edge; this is attributed to the large spin stiffness in this system and boosts confidence in potential spintronics applications of graphene edge magnetism [23]. Although conclusive experimental evidence for edge magnetism is still lacking due to limited control over edge orientation, there has been significant progress in recent years towards the synthesis and characterization of zigzag edges [24–26].

A large number of theoretical studies on graphene edge magnetism represent the interaction by an on-site Hubbard term for simplicity. For the Hubbard model on a honeycomb lattice, arguments in support of edge magnetism [11] can be constructed based on Lieb's theorem [27]. The Coulomb interaction in pristine graphene on a nonmetallic substrate is, nevertheless, poorly screened due to a vanishing density of states at the Dirac points [28,29]. The influence of nonlocal components of the interaction has been investigated both in bulk graphene [30–33] and in restricted geometries [4,8,13,34,35]. (By "nonlocal" we mean having a longer range than on site.) However, many studies on graphene nanoribbons with nonlocal interactions have adopted a mean-field treatment, neglecting fluctuations whose role is especially important in low dimensions [36]. Exact diagonalization has been employed in other studies; despite the light it sheds on the nature of the ground states, correlations in manageably small systems are usually enhanced compared to the thermodynamic limit.

In the present work, we study the effect of long-range interactions on graphene edge ferromagnetism in the limit of weak interactions but beyond the mean-field level. Focusing on a semi-infinite graphene sheet with a single zigzag edge, we find the effective Hamiltonian by projecting the interaction into the Hilbert space of edge states; we then propose a sufficient condition for the maximum spin ferromagnetic multiplet to be the half-filling ground states. Using exact diagonalization, we discuss the possible ground states for interactions in violation of this condition. The long-range Coulomb interaction is shown to satisfy the sufficient condition upon extrapolation to the limit of infinite long-distance cutoff. We also examine the simplest low-energy excitations of the ferromagnetic ground states on a single edge. For short-range interactions, single-particle excitations and single-hole excitations have linear spectra $\propto v\delta k$, where $|\delta k| \ll 1$ is the distance from either Dirac point, with a slope v controlled by the interaction strength. Spin-1 excitons have a small-momentum dispersion that is proportional to $vQ^2 \ln Q$. For the long-range Coulomb interaction, $v \to \infty$, and the dispersion of single-particle or single-hole excitations near the Dirac points scales as $\delta k \ln \delta k$. Finally, for both short-range and Coulomb interactions, a sufficiently large particle-hole symmetry-breaking term in the Hamiltonian can destabilize the ferromagnetic ground state.

II. MODEL

We study a semi-infinite graphene sheet on the xy plane, modeled by a honeycomb lattice which is terminated by an infinite zigzag edge (see Fig. 1). All carbon atoms reside in the half plane $y \geqslant 0$, and the outermost atoms on the zigzag edge (which belong to the A hexagonal sublattice) lie on the x axis. In units of the Bravais lattice constant $a = 2.46$ Å, it is convenient to represent the position of carbon atoms by $\vec{r}_{(m,n)} = (m/2)\hat{x} + (\sqrt{3}n/2)\hat{y}$, where $n \geqslant 0$. While m is always an integer, note that n is an integer only on the A sublattice: for A atoms n and m are both even or both odd, while for B atoms $n + 2/3$ and m are both even or both odd.

The zero modes associated with the zigzag edge are given by [1,2]

$$e_k^\dagger = \frac{1}{\sqrt{2\pi}} \sum_{n\geqslant 0,m} e^{ik\frac{m}{2}} g_n(k) c^\dagger_{m,n,A}, \tag{1}$$

*Corresponding author: zshi@alumni.ubc.ca

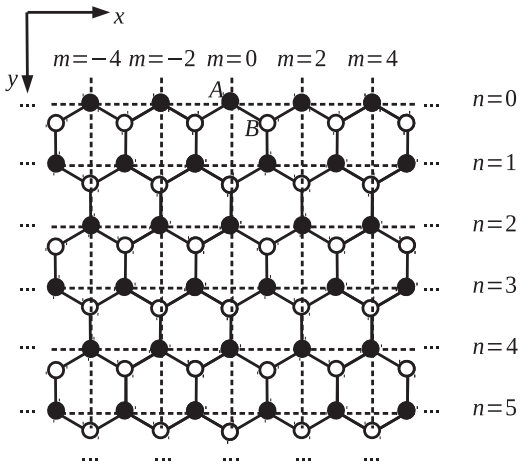

FIG. 1. Sketch of a semi-infinite graphene sheet with a zigzag edge.

where k is the crystal momentum along the edge direction,

$$g_n(k) \equiv \theta\left(k-\frac{2\pi}{3}\right)\theta\left(\frac{4\pi}{3}-k\right)\sqrt{1-4\cos^2\frac{k}{2}}\left(-2\cos\frac{k}{2}\right)^n \tag{2}$$

describes the decay of the wave function into the bulk, and the c operators obey the usual anticommutation relations $\{c_{m,n,A},c^\dagger_{m',n',A}\} = \{c_{m,n,B},c^\dagger_{m',n',B}\} = \delta_{mm'}\delta_{nn'}$, $\{c_{m,n,A},c^\dagger_{m',n',B}\} = 0$. (We have temporarily suppressed the spin index.) These edge states exist only for $2\pi/3 < k < 4\pi/3$, i.e., in 1/3 of the one-dimensional Brillouin zone $0 \leqslant k < 2\pi$. The wave function is nonzero only on the A sublattice and is localized near the zigzag edge. The localization length $\xi_k = -[\ln|2\cos(k/2)|]^{-1}$ vanishes at $k = \pi$ and diverges near the Dirac points $k = 2\pi/3$ and $k = 4\pi/3$.

In addition to the edge states, we also have bulk states which are labeled by k, k_y, and s:

$$b^\dagger_{k,k_y,s} = \frac{1}{2\pi}\frac{1}{\sqrt{2}}\left\{\sum_{n\geqslant 0,m} e^{ik\frac{m}{2}}\left[2i\sin nk_y + \left(2\cos\frac{k}{2}\right)2i\sin(n+1)k_y\right]\frac{t}{E_s(k,k_y)}c^\dagger_{m,n,A} - \sum_{n\geqslant\frac{1}{3},m} e^{ik\frac{m}{2}}\left[2i\sin\left(n+\frac{2}{3}\right)k_y\right]c^\dagger_{m,n,B}\right\}. \tag{3}$$

Here the bulk dispersion relation is

$$E_s(k,k_y) = st\sqrt{\left(2\cos\frac{k}{2}\right)^2 + 1 + 2\left(2\cos\frac{k}{2}\right)\cos k_y}, \tag{4}$$

with nearest-neighbor hopping strength t; k_y is the crystal momentum perpendicular to the edge, $0 \leqslant k_y \leqslant \pi$, and $s = \pm$ is a subband index. Near the Dirac points, where $(k,k_y) = (2\pi/3,\pi) + (\delta k,\delta k_y)$ or $(k,k_y) = (4\pi/3,0) + (\delta k,\delta k_y)$, $E_s(k,k_y)$ takes a Lorentz invariant form $E_s(k,k_y) = st\sqrt{(\delta k_y)^2 + (3/4)(\delta k)^2}$. In this noninteracting model, at zero temperature and half filling, the $s = -$ subband is completely filled and the $s = +$ subband is completely empty. While the edge states are half filled, for the semi-infinite sheet we cannot ascertain which half is filled at this point, unless other ingredients, such as next-nearest-neighbor hopping, edge potential, and electron-electron interaction, are present.

We now introduce a weak repulsive electron-electron interaction. The following extended Hubbard model manifestly respects $SU(2)$ spin symmetry and also particle-hole symmetry at half filling:

$$H_{int} = \frac{1}{2}\sum_{n,m}\sum_{\delta_m,\delta_n} U_{(\delta_m,\delta_n)}\left(\sum_{\sigma=\pm} c^\dagger_{m,n,\sigma}c_{m,n,\sigma} - 1\right) \times \left(\sum_{\sigma'=\pm} c_{m+\delta_m,n+\delta_n,\sigma'}c_{m+\delta_m,n+\delta_n,\sigma'} - 1\right). \tag{5}$$

Here (δ_m,δ_n) runs over all vectors $\vec{\delta} = (\delta_m/2)\hat{x} + (\sqrt{3}\delta_n/2)\hat{y}$ pointing from one lattice site to another; for instance, $U_{(0,0)}$ stands for the strength of the on-site Hubbard interaction, $U_{(0,2/3)}$ is the interaction between nearest-neighbor sites (belonging to different sublattices) in the y direction, $U_{(1,1/3)}$ is the interaction between nearest-neighbor sites at $\pi/6$ angle with the x direction, and $U_{(2,0)}$ is the interaction between next nearest neighbors (belonging to the same sublattice) in the x direction. The sum over n and δ_n is such that both $n \geqslant 0$ and $n + \delta_n \geqslant 0$. To lighten notations, we have suppressed the sublattice indices A and B in this expression because they are uniquely determined by the position indices (m,n) and $(m+\delta_m,n+\delta_n)$.

In general $U_{(\delta_m,\delta_n)} = U_{(-\delta_m,-\delta_n)}$, but apart from this constraint U can be an arbitrary function of δ_m and δ_n. Nevertheless, we further assume that U obeys parity symmetry, $U_{(\delta_m,\delta_n)} = U_{(-\delta_m,\delta_n)}$. For the Hubbard model, $U_{(\delta_m,\delta_n)}$ vanishes unless $\delta_m = \delta_n = 0$. On the other hand, for the unscreened Coulomb interaction, $U_{(\delta_m,\delta_n)}$ is inversely proportional to distance at large distances [8,37,38],

$$U_{(\delta_m,\delta_n)} = U_0\frac{d}{\sqrt{d^2 + |\vec{\delta}|^2}}, \tag{6}$$

where U_0 is the on-site interaction and the half-nearest-neighbor distance $d = 1/(2\sqrt{3})$ accounts for the finite spread of the carbon π orbitals.

Assuming $U_{(\delta_m,\delta_n)} \ll t$, we expect that the low-energy degrees of freedom are composed of the edge states e_k, with $2\pi/3 < k < 4\pi/3$, and the bulk states in the vicinity of the two Dirac points [12,13]. As a first approximation at $O(U)$, we neglect the dynamics of the bulk states completely; they are assumed to be half filled and not spin polarized as in the noninteracting case [7,11]. This approximation allows the projection of the interaction onto the Hilbert space of the edge states. More concretely, we invert Eqs. (1) and (3) to express the c operators in terms of e and b, then take the expectation

values for pairs of b operators using

$$\langle b^\dagger_{k,k_y,-,\sigma} b_{k',k'_y,-,\sigma'}\rangle = \langle b_{k,k_y,+,\sigma} b^\dagger_{k',k'_y,+,\sigma'}\rangle = \delta_{\sigma\sigma'}\delta(k-k')\delta(k_y-k'_y). \quad (7)$$

After some algebra, we find

$$H_{\rm int} = \frac{1}{2}\sum_n \sum_{\delta_m,\delta_n} U_{(\delta_m,\delta_n)} \int_{-\frac{2\pi}{3}}^{\frac{2\pi}{3}} \frac{dq}{2\pi} e^{iq\frac{\delta_m}{2}} O^\dagger_{n+\delta_n}(q) O_n(q), \quad (8)$$

where the sum over (δ_m,δ_n) is now limited to vectors on one of the sublattices; recalling that edge states exist only on the A sublattice, δ_m and δ_n are now both even or both odd. Again, $n \geqslant 0$ and $n+\delta_n \geqslant 0$. $O_n(q)$ is bilinear in e,

$$O_n(q) \equiv \int dk g_n(k+q) g_n(k) \left[\sum_{\sigma=\pm} e^\dagger_{k+q,\sigma} e_{k,\sigma} - \delta(q)\right]. \quad (9)$$

Here q measures the momentum difference between two edge states, so the operator $O_n(q)$ is nontrivial only when $|q| < 2\pi/3$. Note that $O_n(q)$ annihilates all members of the fully polarized ferromagnetic multiplet at half filling for any n and q, which means the ferromagnetic multiplet states are always eigenstates of $H_{\rm int}$ with zero energy.

Due to the constraint on the (δ_m,δ_n) summation, many terms in the interaction (most notably the nearest-neighbor interaction) do not enter the projected effective Hamiltonian in the edge-state subspace, Eq. (8). Although the authors of Ref. [4] predict a charge-polarized ground state when the nearest-neighbor interaction prevails over the on-site interaction, our picture is consistent with their weak-interaction limit, where the charge-polarized state always has a higher energy and the nearest-neighbor interaction is unimportant.

Just like Eq. (5), Eq. (8) manifestly respects $SU(2)$ symmetry and particle-hole symmetry at half filling. In particular, the particle-hole transformation $c_{m,n,\sigma} \to c^\dagger_{m,n,\sigma}$ corresponds to $e_{k,\sigma} \to e^\dagger_{2\pi-k,\sigma}$ and $O_n(q) \to -O_n(q)$ in the edge-state subspace. (The form $e_{k,\sigma} \to e^\dagger_{k,\sigma}$ previously suggested in the Hubbard model [11] is the combination of a particle-hole transformation and a parity transformation.) The particle-hole symmetry is broken by either a weak next-nearest-neighbor hopping $|t_2| \ll t$ in the bulk or a weak potential localized at the edge $|V_e| \ll t$; the latter can arise, for example, at a graphene-graphane interface [7]. When $\Delta = t_2 - V_e \neq 0$, a dispersion develops for the edge states:

$$H = H_{\rm int} + H_\Delta,\ H_\Delta = \Delta \sum_{\sigma=\pm} \int_{\frac{2\pi}{3}}^{\frac{4\pi}{3}} dk (2\cos k + 1) e^\dagger_{k,\sigma} e_{k,\sigma}, \quad (10)$$

assuming the Fermi energy is fixed at the new Dirac point $\epsilon_F = 3t_2$ [7,11].

In the remainder of this paper we analyze the edge-state Hamiltonian given by Eq. (10) at half filling.

III. GROUND STATE

We first study the ground state of the particle-hole symmetric Hamiltonian (8), keeping $\Delta = 0$.

For the projected Hubbard model, it has been proven in Ref. [11] that the fully polarized ferromagnetic multiplet states with maximum total spin are the unique ground states. In the Hubbard case, Eq. (8) becomes

$$H_{\rm int,\ Hubbard} = \frac{1}{2} U \sum_{n=0}^{\infty} \int_{-\frac{2\pi}{3}}^{\frac{2\pi}{3}} \frac{dq}{2\pi} O^\dagger_n(q) O_n(q). \quad (11)$$

It is obvious that $H_{\rm int,\ Hubbard}$ is positive semidefinite. Since the ferromagnetic multiplet states are always zero-energy eigenstates, they must belong to the ground-state manifold of $H_{\rm int,\ Hubbard}$. Furthermore, it is also possible to show that they are the only states annihilated by $O_n(q)$ for any n and q and therefore the unique ground states of $H_{\rm int,\ Hubbard}$ [11]. We emphasize again that the proof rests on the positive semidefiniteness of the Hamiltonian.

Let us explore the extent to which the proof outlined above can be generalized in our extended Hubbard model. In analogy to a semi-infinite tight-binding chain, through the transformation

$$O_n(q) = \int_0^\pi \frac{dK}{\pi} O_K(q) \sin K(n+1), \quad (12)$$

the generic interaction Hamiltonian (8) can be formally diagonalized:

$$H_{\rm int} = \frac{1}{2} \int_{-\frac{2\pi}{3}}^{\frac{2\pi}{3}} \frac{dq}{2\pi} \int_0^\pi \frac{dK}{2\pi} \tilde{U}(k,q) O^\dagger_K(q) O_K(q), \quad (13)$$

where

$$\tilde{U}(K,q) \equiv \sum_{\delta_m,\delta_n} U_{(\delta_m,\delta_n)} \cos(K\delta_n) \cos\frac{q\delta_m}{2}. \quad (14)$$

The spectrum of $\tilde{U}(K,q)$ does not give the spectrum of the interacting problem because $O_K(q)$ does not obey simple commutation relations. Nevertheless, if $\tilde{U}(K,q)$ is positive semidefinite for $0 \leqslant K \leqslant \pi$ and $-2\pi/3 \leqslant q \leqslant 2\pi/3$, we can borrow the arguments from the case of the Hubbard model and show that the ferromagnetic multiplet states are the unique ground states of Eq. (8) at half filling. [That a state is annihilated by all $O_n(q)$ is equivalent to it being annihilated by all $O_K(q)$.] The positive semidefiniteness of $\tilde{U}(K,q)$ is thus a sufficient condition for ferromagnetic ground states.

As a simple example, we consider the model with only on-site and next-nearest-neighbor interactions:

$$U_{(0,0)} \equiv U, \quad U_{(\pm2,0)} \equiv U_{2\parallel}, \quad U_{(\pm1,1)} = U_{(\pm1,-1)} \equiv U_{2\angle}, \quad (15)$$

and $U_{(\delta_m,\delta_n)} = 0$ for other (δ_m,δ_n). (The nearest-neighbor interactions drop out, as noted in Sec. II.) In the next-nearest-neighbor interaction we have introduced an anisotropy between the direction parallel to the edge $U_{2\parallel}$ and the directions at an angle of $\pi/3$ with the edge $U_{2\angle}$. While such anisotropy is not necessarily realistic, we shall see that $U_{2\parallel}$ and $U_{2\angle}$ have very different effects on edge magnetism.

For this model,

$$\tilde{U}(K,q) = U + 2U_{2\parallel}\cos q + 4U_{2\angle}\cos K \cos\frac{q}{2}; \quad (16)$$

as $\cos q/2 > 0$, the minimum of $\tilde{U}$ with respect to K is obtained at $K = \pi$. The positive-semidefiniteness condition

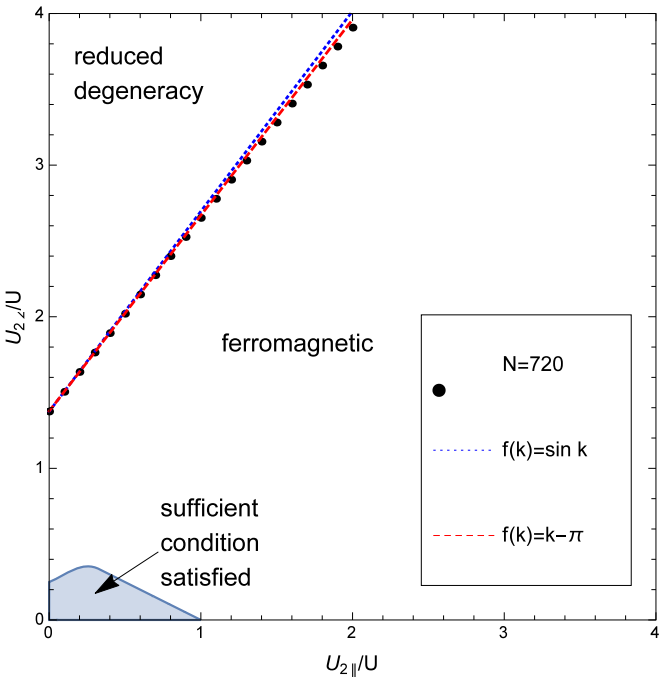

FIG. 2. The ground-state phase diagram of Eq. (15) at half filling on the $U_{2\parallel}/U - U_{2\angle}/U$ plane. The ground states are ferromagnetic below the phase boundary and have reduced degeneracy above the boundary. The boundary is obtained by exact diagonalization in a system with $N = 720$ in the $S_z = N/2 - 1$ sector and is well approximated by the two straight lines corresponding to the trial wave functions $f(k) \propto \sin k$ and $f(k) \propto k - \pi$ (see text). Also shown is the much smaller region where the sufficient condition for ferromagnetic ground states, Eq. (17), is satisfied.

of $\tilde{U}(K,q)$ is therefore equivalent to

$$\forall\, q \in \left[-\frac{2\pi}{3}, \frac{2\pi}{3}\right], U + 2U_{2\parallel}\cos q \geqslant 4U_{2\angle}\cos\frac{q}{2}. \quad (17)$$

This is a sufficient condition for the ground states to be ferromagnetic in the model specified by Eq. (15). It requires that neither $U_{2\parallel}$ nor $U_{2\angle}$ should be greater than U. In particular, Eq. (17) becomes $U_{2\angle} \leqslant U/4$ when $U_{2\parallel} = 0$ and $U_{2\parallel} \leqslant U$ when $U_{2\angle} = 0$; in the isotropic case $U_{2\parallel} = U_{2\angle} \equiv U_2$, Eq. (17) is reduced to $U_2 \leqslant U/3$.

It is natural to wonder whether the fully polarized ferromagnetic multiplet remains the ground states of Eq. (15) at half filling when the sufficient condition (17) is violated. To answer the question we perform exact diagonalization on Eq. (15). Assuming a system size of L unit cells along the edge, the number of different edge-state momenta allowed is approximately $N = L/3$. It is convenient to take advantage of the good quantum numbers of the Hamiltonian, namely, the z component of the total spin S_z and also the total momentum Q along the edge direction [13]. We measure Q relative to the fully polarized state $|\mathrm{FM}\uparrow\rangle$ where every edge state is singly occupied by a spin-up electron; for this state $S_z = N/2$ and $Q = 0$.

In Fig. 2 we plot the ferromagnetic phase boundary for Eq. (15) on the $U_{2\parallel} - U_{2\angle}$ plane, obtained from exact diagonalization. For comparison we also show the region where the sufficient condition (17) is satisfied. In most of the parameter space, we find that the ground states at half filling are uniquely given by the $(N+1)$-fold-degenerate ferromagnetic multiplet with $S_z = -N/2, -N/2+1, \ldots, N/2$ and $Q = 0$. In particular, the ground states are always ferromagnetic in the isotropic case $U_{2\parallel} = U_{2\angle}$. However, in the region above the phase boundary where $U_{2\angle}$ is relatively large compared to both U and $U_{2\parallel}$, the ground states are not part of the ferromagnetic multiplet, but rather form a negative-energy manifold with a lower degeneracy and a lower total spin. For fixed U and $U_{2\parallel}$, the degeneracy is reduced as $U_{2\angle}$ gradually increases, and eventually, for sufficiently large $U_{2\angle}$ the ground state becomes a nondegenerate singlet state in the $S_z = 0$ sector.

In Fig. 3, choosing a fixed $U_{2\parallel}/U$, we plot $E_{\mathrm{GS}}(S_z)$ (the ground-state energy in the sector labeled by S_z) as a function

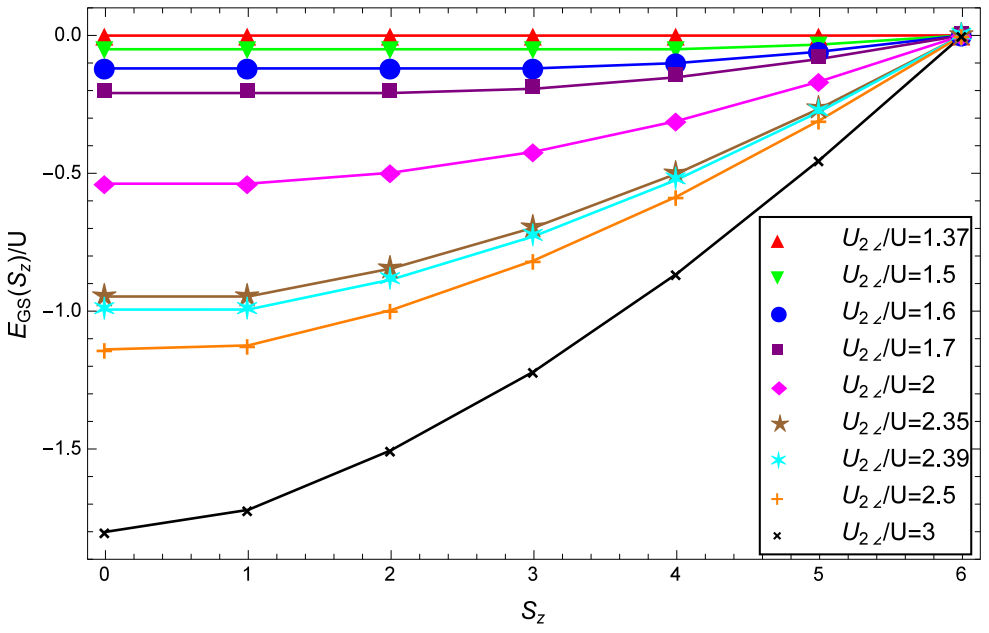

FIG. 3. The ground-state energy in the S_z sector $E_{GS}(S_z)$ versus $|S_z|$ for $U_{2\parallel} = 0$ and various $U_{2\angle}/U$ outside of the ferromagnetic regime. The results are obtained by exact diagonalization in a system with $N = 12$.

of $|S_z|$ for different $U_{2\angle}/U$ outside of the ferromagnetic regime. We observe that $E_{\rm GS}(S_z)$ is a monotonically increasing function of $|S_z|$ in general and becomes a strictly increasing function of $|S_z|$ if $U_{2\angle}$ is sufficiently large. This property of $E_{\rm GS}(S_z)$ allows us to determine the ferromagnetic phase boundary in Fig. 2 by calculating $E_{\rm GS}(S_z = N/2-1)$, which for a given N is considerably less numerically intensive than $E_{\rm GS}(S_z = 0)$. Reasonably accurate estimates of the phase boundary can then be made through a variational calculation. We can characterize an arbitrary $Q = 0$ state in the $S_z = N/2-1$ sector by

$$\int_{\frac{2\pi}{3}}^{\frac{4\pi}{3}} dk f(k) e_{k,\uparrow} e^{\dagger}_{k,\downarrow} |\mathrm{FM}\uparrow\rangle. \tag{18}$$

The ferromagnetic state in this sector corresponds to $f(k) = 1$, i.e., an equal-weighted superposition of all states where every edge state is singly occupied. The energy expectation value as a functional of f is a linear combination of U, $U_{2\|}$, and $U_{2\angle}$:

$$E[f] = UC_0[f] + U_{2\|}C_{2\|}[f] + U_{2\angle}C_{2\angle}[f]. \tag{19}$$

If $E[f] < 0$, the ground states cannot be the ferromagnetic multiplet whose energy is always zero. For $f(k) \propto \sin k$, $C_0 = 0.100$, $C_{2\|} = 0.0964$, and $C_{2\angle} = -0.0730$; for $f(k) \propto k - \pi$, $C_0 = 0.0946$, $C_{2\|} = 0.0887$, and $C_{2\angle} = -0.0687$. For these two trial wave functions, the trajectories above which $E[f] < 0$ are plotted in Fig. 2; both trajectories are very close to the ferromagnetic phase boundary obtained from exact diagonalization.

It should also be cautioned that anisotropy is not necessary to stabilize nonferromagnetic ground states. For instance, we can also study an isotropic interaction consisting of an on-site term and six fifth-nearest-neighbor terms (or, equivalently, next-nearest-neighbor terms on the same sublattice):

$$U_{(0,0)} \equiv U, \quad U_{(0,\pm 2)} = U_{(\pm 3,1)} = U_{(\pm 3,-1)} \equiv U_5, \tag{20}$$

and $U_{(\delta_m,\delta_n)} = 0$ for other (δ_m,δ_n). For this model

$$\tilde{U}(K,q) = U + 2U_5\left(\cos 2K + 2\cos K \cos\frac{3q}{2}\right), \tag{21}$$

so our sufficient condition for ferromagnetism becomes $U_5 \leqslant U/3$. In a system with $N = 720$, exact diagonalization shows that a nonferromagnetic ground state appears when $U_5 > 80.48U$, i.e., when the nonlocal U_5 term is far stronger than the on-site interaction.

Our exact diagonalization results for both models indicate that while ferromagnetism is favored by the on-site interaction, it may be destabilized by sufficiently strong nonlocal interactions. This is in agreement with the findings of Ref. [33] that the effective on-site part of the interaction in bulk graphene is reduced by a weighted average of nonlocal interactions.

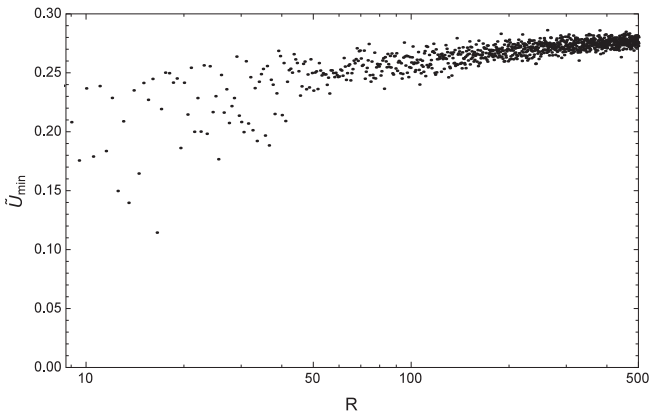

FIG. 4. The minimum of $\tilde{U}(K,q)$ for $0 \leqslant K \leqslant \pi$ and $-2\pi/3 \leqslant q \leqslant 2\pi/3$, $\tilde{U}_{\rm min}$, versus R, the long-distance cutoff introduced artificially in the Coulomb interaction Eq. (6).

We now investigate whether the unscreened Coulomb interaction, Eq. (6), satisfies the sufficient condition for ferromagnetism. To this end, we introduce a long-distance cutoff R and minimize $\tilde{U}(K,q)$ for the interaction that is given by Eq. (6) for $|\vec{\delta}| \leqslant R$ but vanishes for $|\vec{\delta}| > R$. In Fig. 4 we show $\tilde{U}_{\rm min}$, the minimum of $\tilde{U}(K,q)$ for $0 \leqslant K \leqslant \pi$ and $-2\pi/3 \leqslant q \leqslant 2\pi/3$, as a function of R for $R \leqslant 500$. While $\tilde{U}_{\rm min}$ oscillates wildly, its lower envelope is an increasing function of R, and $\tilde{U}_{\rm min}$ does not go below $0.2U_0$ for $50 \leqslant R \leqslant 500$. This strongly implies that $\tilde{U}_{\rm min}$ remains positive as $R \to \infty$ and provides evidence that the ferromagnetic multiplet states are the unique ground states for the unscreened Coulomb interaction.

A remark is in order about the short-distance cutoff $d = 1/(2\sqrt{3})$ in Eq. (6). If d is treated as a tunable parameter of our model, then the observation that $\tilde{U}_{\rm min}(R \to \infty) > 0$ is valid only when $d \lesssim 1$. If d is close to 1, $\tilde{U}_{\rm min}$ oscillates around zero even for R up to 500. Nevertheless, as shown in the next-nearest-neighbor model and the fifth-nearest-neighbor model, violation of the sufficient condition for ferromagnetism $\tilde{U}_{\rm min} \geqslant 0$ is not an indication of ground states being nonferromagnetic. Indeed, we have verified in the $S_z = N/2-1$ sector that the ground states remain ferromagnetic for R up to 20 and d up to 10.

IV. LOW-ENERGY EXCITATIONS

In this section we discuss the low-energy single-particle, single-hole, and particle-hole excitations of the ferromagnetic ground state and also the effect of the particle-hole symmetry-breaking term Δ.

It is simplest to consider the excitations from the maximum S_z state $|\mathrm{FM}\uparrow\rangle$. We can rewrite the projected Hamiltonian of Eq. (10) in a form which explicitly annihilates $|\mathrm{FM}\uparrow\rangle$:

$$H_{\rm int} = \int dk[\epsilon_p(k) e^{\dagger}_{k,\downarrow} e_{k,\downarrow} + \epsilon_h(k) e_{k,\uparrow} e^{\dagger}_{k,\uparrow}] - \int \frac{dkdk'dq}{2\pi} \Gamma(k,k',q) e_{k,\uparrow} e^{\dagger}_{k'-q,\downarrow} e_{k',\downarrow} e^{\dagger}_{k+q,\uparrow}$$
$$+ \frac{1}{2}\int \frac{dkdk'dq}{2\pi} \Gamma(k,k',q)(e^{\dagger}_{k+q,\downarrow} e^{\dagger}_{k'-q,\downarrow} e_{k',\downarrow} e_{k,\downarrow} + e_{k+q,\uparrow} e_{k'-q,\uparrow} e^{\dagger}_{k',\uparrow} e^{\dagger}_{k,\uparrow}), \tag{22}$$

where the domains of integration are such that all edge states have momenta between $2\pi/3$ and $4\pi/3$, the interaction kernel is

$$\Gamma(k,k',q) = \frac{g_0(k)g_0(k')g_0(k+q)g_0(k'-q)}{1-16\cos\frac{k}{2}\cos\frac{k+q}{2}\cos\frac{k'}{2}\cos\frac{k'-q}{2}}\frac{1}{2}\sum_{\delta_m,\delta_n} U_{(\delta_m,\delta_n)}\cos\frac{q\delta_m}{2}\left[\left(4\cos\frac{k'}{2}\cos\frac{k'-q}{2}\right)^{|\delta_n|}+\left(4\cos\frac{k}{2}\cos\frac{k+q}{2}\right)^{|\delta_n|}\right], \tag{23}$$

and the energy to create one single spin-down electron or one single spin-up hole is

$$\epsilon_{p/h}(k) = \frac{1}{2}\int_{\frac{2\pi}{3}}^{\frac{4\pi}{3}}\frac{dk'}{2\pi}\Gamma(k,k',k'-k) \pm \Delta(2\cos k+1). \tag{24}$$

As noted in Refs. [11,12], the interaction $\Gamma(k,k',q)$ is strongly momentum dependent. For both Hubbard and Coulomb interactions, $\Gamma(k,k',q)$ is positive, so that spin-down electrons attract spin-down holes, which favors the formation of bound states between the two. The third term in Eq. (22) generally gives rise to interaction between edge states with the same spin orientation, although for the Hubbard model it vanishes due to an additional symmetry of the kernel, $\Gamma(k,k',q) = \Gamma(k,k',k'-k-q)$.

A. Single-particle and single-hole excitations

We first examine the eigenstates deviating slightly from half filling, namely, the single-particle excitations and single-hole excitations. They are represented by $e^\dagger_{k,\downarrow}|\mathrm{FM}\uparrow\rangle$ [of energy $\epsilon_p(k)$] and $e_{k,\uparrow}|\mathrm{FM}\uparrow\rangle$ [of energy $\epsilon_h(k)$], respectively. Using the definitions (24) and (23) and the fact that $\delta_n+\delta_m$ is even, it is easy to show that $\epsilon_{p/h}(k) = \epsilon_{p/h}(2\pi-k)$, so we may focus on $2\pi/3 \leqslant k \leqslant \pi$.

Near the Dirac point $0 < k-2\pi/3 \ll 1$, we can expand Eq. (24) to obtain

$$\epsilon_{p/h}(k) \approx (v \mp \sqrt{3}\Delta)\left(k-\frac{2\pi}{3}\right), \tag{25}$$

where the velocity v depends only on the interactions:

$$v \equiv \frac{\sqrt{3}}{2}\sum_{\delta_m,\delta_n} U_{(\delta_m,\delta_n)}\int_{\frac{2\pi}{3}}^{\frac{4\pi}{3}}\frac{dk'}{2\pi}\left(2\cos\frac{k'}{2}\right)^{|\delta_n|}\cos\left(k'-\frac{2\pi}{3}\right)\frac{\delta_m}{2}. \tag{26}$$

Since the k' integral is finite, v is finite for any short-range interaction. Equation (25) shows that, as in the projected Hubbard model [11], the single-particle and single-hole excitations are generally gapless at the Dirac points for a single zigzag edge.

For the next-nearest-neighbor model (15), v is always positive:

$$v = \frac{\sqrt{3}}{6}U + \frac{3}{4\pi}U_{2\parallel} + \left(\frac{1}{\sqrt{3}}-\frac{3}{2\pi}\right)U_{2\angle}. \tag{27}$$

Nevertheless, v may become negative for certain strongly nonlocal interactions. An example is the term with $\delta_m = 4$ and $\delta_n = 0$, which gives a coefficient of $-3/(16\pi)$. The ferromagnetic ground state will be unstable against the creation of electrons or holes near the Dirac points in the case of $v < 0$, or, more generally, $v < \sqrt{3}|\Delta|$, when the particle-hole symmetry-breaking term Δ is nonzero.

The case of unscreened Coulomb interaction (6) is especially interesting. In this case the low-energy behavior of $\epsilon_{p/h}(k)$ is controlled by the long -range part of $U_{(\delta_m,\delta_n)}$. When $|\delta_n| \gg 1$ or $|\delta_m| \gg 1$, the k' integral is dominated by k' near the Dirac points, and we find [39]

$$\begin{aligned}&\int_{\frac{2\pi}{3}}^{\frac{4\pi}{3}}\frac{dk'}{2\pi}\left(2\cos\frac{k'}{2}\right)^{|\delta_n|}\cos\left(k'-\frac{2\pi}{3}\right)\frac{\delta_m}{2}\\ &\quad\approx \frac{1}{2\pi}\mathrm{Re}\left[\frac{2}{\sqrt{3}|\delta_n|-i\delta_m}+(-1)^{|\delta_n|}e^{i\frac{\pi}{3}\delta_m}\frac{2}{\sqrt{3}|\delta_n|+i\delta_m}\right].\end{aligned} \tag{28}$$

Approximating the sum over δ_n and δ_m by integrals over $x = \delta_m/2$ and $y = \sqrt{3}\delta_n/2$ and discarding the subleading contribution from the oscillating term, we see that $v \propto \ln R$, where R is the long-distance cutoff:

$$\begin{aligned}v &\approx \int dx\int dy\,\frac{U_0 d}{\sqrt{x^2+y^2}}\frac{1}{2\pi}\frac{|y|}{x^2+y^2}\\ &\approx \frac{U_0 d}{2\pi}\int_0^{2\pi}d\theta|\sin\theta|\int_d^R\frac{dr}{r} = \frac{2U_0 d}{\pi}\ln\frac{R}{d}.\end{aligned} \tag{29}$$

As $R\to\infty$, the only other large distance scale in the problem is given by the inverse distance to the Dirac points, which should therefore replace R as the distance cutoff. In other words, for the unscreened Coulomb interaction, $\epsilon_{p/h}$ has the following behavior for $0 < k-2\pi/3 \ll 1$:

$$\epsilon_{p/h}(k) \approx \frac{2U_0 d}{\pi}\left(k-\frac{2\pi}{3}\right)\ln\frac{\Lambda}{k-\frac{2\pi}{3}}, \tag{30}$$

where $\Lambda \ll 1$ is a momentum cutoff. This behavior is not affected by the particle-hole symmetry-breaking term Δ, which merely shifts Λ.

In Fig. 5 we plot $\epsilon_{p/h}(k)/(k-2\pi/3)$ versus $\ln(k-2\pi/3)$ at $0 < k-2\pi/3 \ll 1$ for the Coulomb interaction with various R and show how the logarithmic divergence in Eq. (30) is cut off at low energies by R. We also plot the velocity v given by Eq. (26) as a function of $\ln R$ in Fig. 6. These results suggest that the Coulomb interaction produces a divergent "Fermi velocity" for edge modes near the Dirac points, a behavior reminiscent of the marginal Fermi liquid in bulk graphene with Coulomb interaction [40].

It is also useful to consider $k = \pi$ since this is where $\epsilon_{p/h}(k)$ obtains its maximum for the Hubbard interaction and the Coulomb interaction in the absence of particle-hole symmetry breaking. At $k = \pi$ Eq. (24) is again greatly

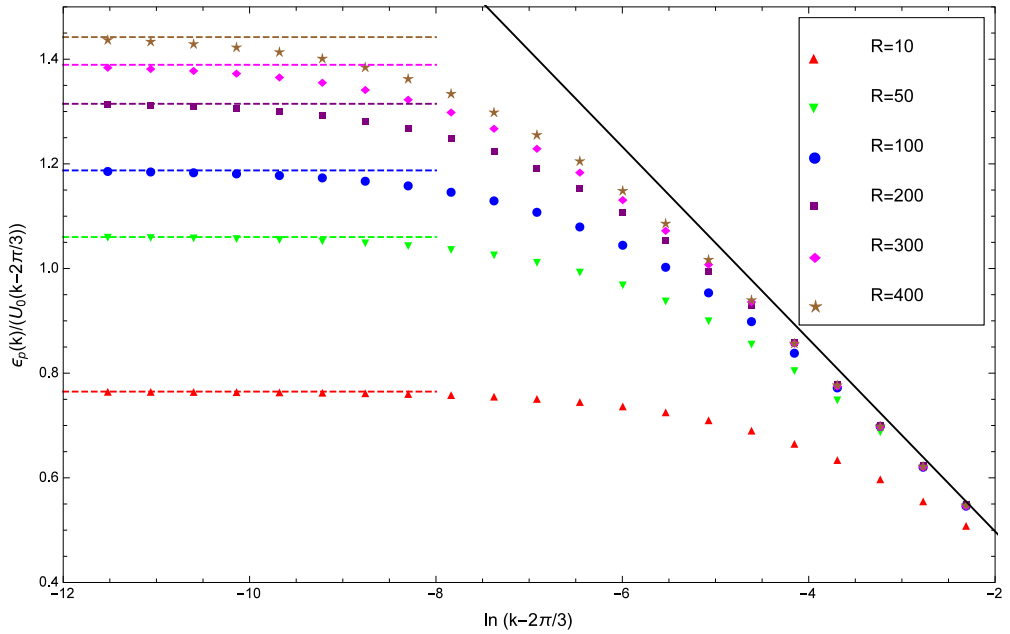

FIG. 5. The single-particle/single-hole dispersion for the Coulomb interaction near the Dirac point. $\epsilon_{p/h}(k)/[U_0(k-2\pi/3)]$ is plotted against $\ln(k-2\pi/3)$ for $10^{-5} \leqslant k-2\pi/3 \leqslant 0.1$ and different values of long-distance cutoff R, with the particle-hole symmetry-breaking perturbation Δ set to zero. For comparison we also show the velocity given by Eq. (26) for each R as a horizontal line. The black line has a slope of $2d/\pi$.

simplified:

$$\epsilon_{p/h}(\pi) = \mp\Delta + \left(\frac{\sqrt{3}}{2\pi} - \frac{1}{6}\right)U_{(0,0)} + \left(\frac{1}{6} - \frac{\sqrt{3}}{8\pi}\right)U_{(1,0)} + \frac{1}{\pi}{\sum_{\delta_m}}' U_{(\delta_m,0)}\left[\frac{8}{\delta_m(\delta_m^2-4)}\sin\frac{\pi}{6}\delta_m - \frac{4\sqrt{3}}{\delta_m^2-4}\cos\frac{\pi}{6}\delta_m\right], \tag{31}$$

where the sum is over even δ_m with $\delta_m \geqslant 4$.

Also, $\epsilon_{p/h}(\pi)$ is finite for any short-range interaction. Interestingly, $\epsilon_{p/h}(\pi)$ depends on $U_{(\delta_m,\delta_n)}$ only if $\delta_n = 0$: it is, for instance, independent of $U_{2\angle}$ in the next-nearest-neighbor model (15). For the Coulomb interaction (6), the δ_m sum turns out to be convergent, and we find

$$\epsilon_{p/h}(\pi) \approx \mp\Delta + 0.189U_0, \tag{32}$$

where U_0 is the on-site interaction strength. Therefore, when $\Delta > \Delta_c(R\to\infty) = 0.189U_0$ for the unscreened Coulomb interaction, the maximum S_z state $|\,\mathrm{FM}\uparrow\rangle$ becomes unstable towards the creation of a spin-down electron at $k=\pi$, e.g., by absorption from the bulk. [For Hubbard interaction with strength U, the condition is $\Delta > \Delta_c(R=0) = (\sqrt{3}/(2\pi) - 1/6)U \approx 0.109U$ [11].] Similarly, when $\Delta < -\Delta_c(R\to\infty)$, there is an instability towards the creation of a spin-up hole at $k=\pi$.

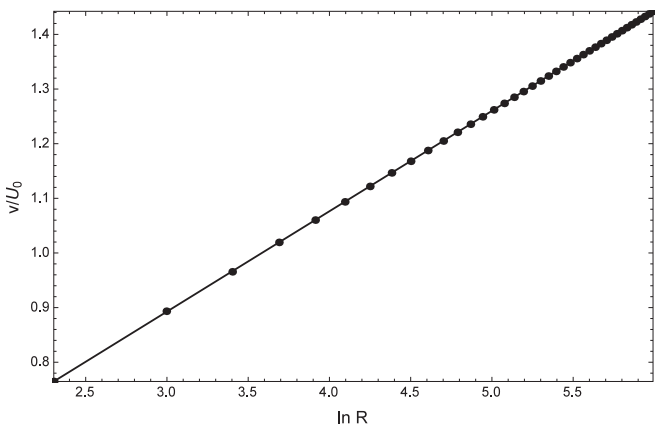

FIG. 6. The velocity given by Eq. (26) for the Coulomb interaction as a function of the long-distance cutoff R. The fitted line has a slope of 0.1836 while $2d/\pi = 0.1838$.

In Fig. 7 we plot $\epsilon_p(k)$ versus k for $2\pi/3 \leqslant k \leqslant 4\pi/3$ for the Coulomb interaction with different values of long-distance cutoff R, both when $\Delta = 0$ and when $\Delta = \Delta_c(R)$, so that $\epsilon_p(\pi)$ vanishes. Notice that for the Coulomb interaction $\epsilon_p(k) > 0$ for $0 < k - 2\pi/3 \ll 1$ even when $\Delta = \Delta_c(R)$; that is, as we increase $|\Delta|$, single-particle or single-hole creation energy becomes negative at $k=\pi$ sooner than it does near the Dirac points.

B. One-particle-one-hole sector

We turn to the half-filled sector with $N-1$ spin-up electrons and one spin-down electron, so that $S_z = N/2 - 1$. This sector hosts one spin-down electron and one spin-up hole relative to the $|\mathrm{FM}\uparrow\rangle$ state and accommodates the excitations that would be seen as magnons in an effective spin model.

Let the total momentum relative to $|\mathrm{FM}\uparrow\rangle$ be Q, and without loss of generality we assume $Q \geqslant 0$. Denoting an

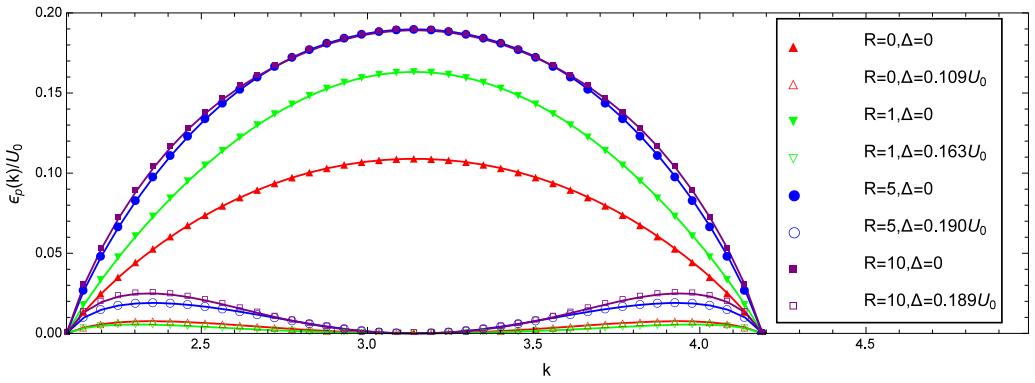

FIG. 7. The single-particle dispersion for the Coulomb interaction. $\epsilon_p(k)/U_0$ is plotted against k for $2\pi/3 \leqslant k \leqslant 4\pi/3$ and different values of long-distance cutoff R. The particle-hole symmetry-breaking perturbation Δ is either zero (solid symbols) or $\Delta_c(R)$ (open symbols).

eigenstate by

$$\int_{\frac{2\pi}{3}}^{\frac{4\pi}{3}-Q} dk f(k;Q) e_{k,\uparrow} e^{\dagger}_{k+Q,\downarrow} |\mathrm{FM}\uparrow\rangle, \tag{33}$$

we obtain the following Schrödinger's equation:

$$[E-\epsilon_h(k)-\epsilon_p(k+Q)]f(k;Q) = -\int \frac{dk'}{2\pi}\Gamma(k,k'+Q,k'-k)f(k';Q), \tag{34}$$

where E is the energy eigenvalue. The ferromagnetic state in the one-particle-one-hole sector, $f(k;Q=0)=1$, is obviously a zero-energy solution.

It is possible for $f(k,Q)$ to have a δ-function peak at $k=k_0$. In this case the solution to Eq. (34) is part of the one-particle-one-hole continuum and has an energy $E=\epsilon_h(k_0)+\epsilon_p(k_0+Q)$. Another possibility is having $E<\epsilon_h(k)+\epsilon_p(k+Q)$ for any k, in which case $f(k;Q)$ does not have any δ-function peaks, and the solution is a particle-hole bound state or an exciton. Since it reduces S_z by 1, it can also be viewed as a magnon in an effective spin model.

For any short-range interaction, we can show that the exciton energy has the following $Q \ll 1$ behavior:

$$E(Q) = \frac{3v}{2\pi}\left(1-\frac{3\Delta^2}{v^2}\right)Q^2 \ln\frac{\Lambda'}{Q}, \tag{35}$$

where v is the velocity equation (26) that also appears in the single-particle dispersion and $\Lambda' \ll 1$ is again a momentum cutoff. The inverse exciton mass, or the spin stiffness of the ferromagnetic zigzag edge, is therefore logarithmically divergent. The derivation of Eq. (35) is sketched in the Appendix, where we see the divergence arises due to the linear behavior of $\epsilon_{p/h}(k)$ near the Dirac points. This divergence is possibly related to the large spin stiffness found by Refs. [6,22] for U comparable to t.

Although similar exciton dispersions have been previously reported in carbon nanotubes [41], in contrast to Eq. (35) they originate from the long-range nature of the Coulomb interaction. In fact, since in the Coulomb interaction with a long-distance cutoff R we have $v \propto \ln R$, we expect that Eq. (35) is modified to $E(Q) \propto Q^2 \ln^2 Q$ for $R \to \infty$; that is, the spin stiffness is even more divergent than a logarithm for the unscreened Coulomb interaction.

Figure 8 shows $E(Q)/Q^2$ plotted against $\ln Q$ at $0 < Q \ll 1$ for some values of R and $\Delta = 0$, where $E(Q)$ is found by solving Eq. (34) numerically via Chebyshev series expansion [42].

It is also helpful to examine the effect of Δ on the exciton dispersion, taking as an example the Coulomb interaction with a long-distance cutoff R. As depicted in Fig. 9, when $|\Delta| = \Delta_c(R)$ so that $\epsilon_p(\pi) = 0$, the exciton dispersion $E(Q)$ calculated numerically also approximately vanishes at $Q = \pm\pi/3$, and the exciton wave function strongly favors the state with a spin-down electron at π and a spin-up hole at either Dirac point. For $|\Delta| > \Delta_c(R)$, in parallel with the Hubbard case [11], $E(\pm\pi/3)$ becomes negative, which indicates that the ground state at half filling is no longer maximally spin polarized; instead, the edge states near π become more likely to be doubly occupied, and the edge states near the Dirac points become more likely to be unoccupied.

Finally, we mention that in the two-particle-two-hole sector, the excitons in the one-particle-one-hole sector can form an additional bound state below the exciton continuum. Nevertheless, for both the Hubbard and the Coulomb interactions with $|\Delta| < \Delta_c(R)$, we find numerically that the bottom of the two-particle-two-hole bound-state dispersion remains positive; we thus conjecture that the ferromagnetic ground state is stable for $|\Delta|$ up to $\Delta_c(R)$. We also mention that the bound-state picture provides an intuitive explanation for the nonferromagnetic regime in Fig. 3: for $M < N/2$, we can usually form an M-particle-M-hole bound state with a non-negative binding energy, i.e., with an energy lower than or equal to the sum of energies of an $(M-1)$-particle-$(M-1)$-hole bound state and a one-particle-one-hole bound state. Therefore, if the one-particle-one-hole ground state has a negative energy as happens for sufficiently large $U_{2\angle}$, then as M increases and $|S_z|$ decreases, the ground-state energy in the S_z sector either stays the same or decreases.

V. DISCUSSION AND CONCLUSIONS

In our effective model (8) at $O(U)$, we have ignored the dynamics of low-lying bulk degrees of freedom near the Dirac points, so an obvious issue is whether this approximation is justified. For the on-site Hubbard interaction, the answer is partly given by Refs. [11,43], where effective Hamiltonians

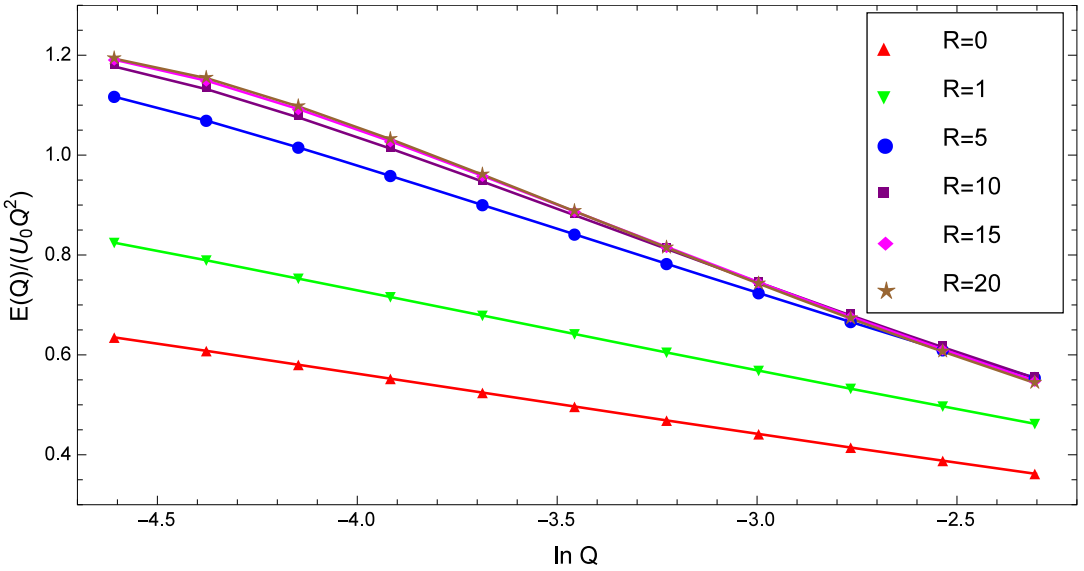

FIG. 8. The exciton dispersion for the Coulomb interaction at small momenta. $E(Q)/(U_0Q^2)$ is plotted against $\ln Q$ for $0.01 \leqslant Q \leqslant 0.1$ and different values of long-distance cutoff R, with the particle-hole symmetry-breaking perturbation Δ set to zero. The lowest 100 Chebyshev polynomials are retained in the numerical solution.

are found to $O(U^2/t)$ by integrating out the bulk states and neglecting retardation. While Ref. [11] finds that the $O(U^2/t)$ correction to the Hamiltonian has a $q^2 \ln q$ behavior for small momentum transfer q, such behavior does not necessarily hint at a breakdown of the perturbation theory, as logarithms also appear at $O(U)$, e.g., in the exciton dispersion equation (35). Reference [43] further shows that, as far as the effective spin model is concerned, the interaction strengths are only weakly modified by the bulk states even for U comparable to t. In other words, there is no evidence that the perturbation theory in U/t is divergent. However, while a weak Hubbard interaction is known to be irrelevant in the bulk, a weak Coulomb interaction is marginally irrelevant and may lead to further logarithmic corrections [29,40]. It therefore remains an open question whether integrating out the bulk states at $O(U^2/t)$ qualitatively changes the physics of the $O(U)$ edge model for the unscreened Coulomb interaction.

Another problem that we have not discussed so far is the interedge coupling in realistic graphene nanoribbons. We now consider a ribbon of large but finite width $W \gg 1$ with two zigzag edges, whose overall ground state is antiferromagnetic. The interedge coupling originates in part from the direct interaction between opposite edges, which is significant even at the first order in interaction if it is long range [$O(U_0/W)$ in the Coulomb case]. Interedge coupling is also mediated by bulk states, which is second order in interaction and is $O(U^2/(tW^2))$ in the Hubbard case [11]. Yet another source is the hopping amplitude between edge states of opposite edges, which exists even in the absence of interactions and leads to an energy gap exponentially small in W. For wide ribbons $W \gg 1$, it is well known that the edge states are no longer strictly localized near one edge when their momenta are within $O(1/W)$ of the Dirac points. The hopping amplitude at momentum k thus grows rapidly as k approaches the

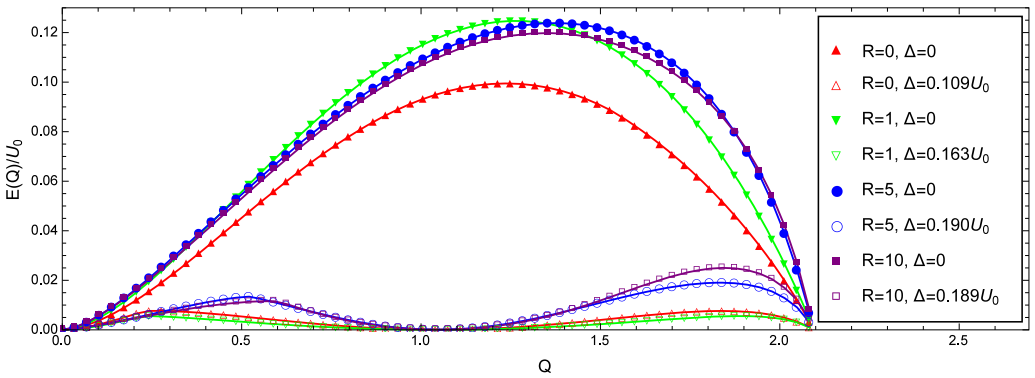

FIG. 9. The exciton dispersion for the Coulomb interaction. $E(Q)/U_0$ is plotted against Q for $0 \leqslant Q \leqslant 2\pi/3$ and different values of long-distance cutoff R. The particle-hole symmetry-breaking perturbation Δ is either zero (solid symbols) or $\Delta_c(R)$ (open symbols). The lowest 100 Chebyshev polynomials are retained in the numerical solution.

Dirac points, eventually reaching $O(t/W)$ [5,44]. Under our assumption $U \ll t$, this is actually a much larger energy scale than that of the direct interedge Coulomb interaction or that of the bulk-mediated interedge interaction. Thus it is not justified to ignore the interedge hopping amplitude near the Dirac points in the effective model for a nanoribbon. In fact, at the mean-field level, it is exactly the part of the Brillouin zone near the Dirac points that contributes the most to the interedge superexchange interaction [5,8], and the spin-wave dispersion becomes linear for small momenta once the interedge coupling is taken into account [9]. Although an effective edge model incorporating the interedge hopping [12] is often much less analytically accessible beyond the mean-field level, we hope further insight on the effect of Coulomb interaction in finite-width nanoribbons can be gleaned from exact diagonalization.

In conclusion, we have investigated the effects of long-range interactions on the zigzag edge states of a semi-infinite graphene sheet. By projecting the interaction onto the edge-state subspace, we obtain an effective model for which the states in the maximally polarized ferromagnetic multiplet are zero-energy eigenstates. A sufficient condition is found for the ferromagnetic multiplet to be the ground states, and we presented evidence that the unscreened Coulomb interaction satisfies this condition, which implies that its ground states are ferromagnetic. In cases where the sufficient condition is not met, exact diagonalization results indicate that the ground state can be nonferromagnetic, provided that certain nonlocal components of the interaction are sufficiently strong. We also discussed the single-particle excitations, single-hole excitations, and spin-1 excitons of the maximum S_z ground state. For short-range interactions the single-particle and single-hole excitations have linear dispersions near the Dirac points, as described in Eq. (25). The slope v also governs the exciton energy at small momenta, Eq. (35), which shows a $vQ^2 \ln Q$ behavior. For the unscreened Coulomb interaction v becomes logarithmically divergent as a function of the long-distance cutoff, corresponding to a $\delta k \ln \delta k$ behavior, where $\delta k \ll 1$ is the distance from either of the Dirac points. The edge states acquire a dispersion due to a particle-hole symmetry-breaking perturbation Δ; the ferromagnetic ground state can be destroyed if $|\Delta|$ is large enough.

ACKNOWLEDGMENTS

This work was supported in part by NSERC of Canada, Discovery Grant No. 04033-2016, and the Canadian Institute for Advanced Research. Z.S. would like to acknowledge helpful discussions with T. Liu and E. Nica.

APPENDIX: EXCITON DISPERSION AT SMALL MOMENTA FOR A SINGLE ZIGZAG EDGE WITH SHORT-RANGE INTERACTIONS

For simplicity, we illustrate the derivation of Eq. (35) with the Hubbard interaction $U_{(0,0)} = U$. Generalization to nonlocal interactions is tedious but straightforward; it is briefly discussed at the end of this appendix.

Expanding the denominator of the kernel Γ in Eq. (34), we can isolate the k dependence of $f(k;Q)$:

$$f(k;Q) = -\frac{g_0(k)g_0(k+Q)}{E-\epsilon_h(k)-\epsilon_p(k+Q)} \sum_{l=0}^{\infty} \left(4\cos\frac{k}{2}\cos\frac{k+Q}{2}\right)^l U\Phi_l(Q), \tag{A1}$$

where Φ's are independent of k and are defined as

$$\Phi_l(Q) = \int_{\frac{2\pi}{3}}^{\frac{4\pi}{3}-Q} \frac{dk'}{2\pi} g_0(k'+Q)g_0(k') \left(4\cos\frac{k'}{2}\cos\frac{k'+Q}{2}\right)^l f(k';Q). \tag{A2}$$

Inserting Eq. (A1) into Eq. (A2), we obtain an infinite number of linear equations satisfied by Φ:

$$\begin{aligned}\Phi_l(Q) = &-\int \frac{dk'}{2\pi} \frac{\left(1-4\cos^2\frac{k'+Q}{2}\right)\left(1-4\cos^2\frac{k'}{2}\right)}{E-\epsilon_h(k')-\epsilon_p(k'+Q)} \left(4\cos\frac{k'}{2}\cos\frac{k'+Q}{2}\right)^l \\ &\times \sum_{l'=0}^{\infty} \left(4\cos\frac{k'}{2}\cos\frac{k'+Q}{2}\right)^{l'} U\Phi_{l'}(Q).\end{aligned} \tag{A3}$$

For $Q \ll 1$, the integrand on the right-hand side can be expanded to $O(E)$ and $O(Q^2)$.

$$\begin{aligned}\Phi_l(Q) = &\int \frac{dk'}{2\pi} \frac{\left(1-4\cos^2\frac{k'}{2}\right)^2}{\epsilon_h(k')+\epsilon_p(k')} \left(4\cos^2\frac{k'}{2}\right)^l \sum_{l'=0}^{\infty} \left(4\cos^2\frac{k'}{2}\right)^{l'} U\Phi_{l'}(Q) \\ &+ E\int \frac{dk'}{2\pi} \frac{\left(1-4\cos^2\frac{k'}{2}\right)^2}{[\epsilon_h(k')+\epsilon_p(k')]^2} \left(4\cos^2\frac{k'}{2}\right)^l \sum_{l'=0}^{\infty} \left(4\cos^2\frac{k'}{2}\right)^{l'} U\Phi_{l'}(0) \\ &+ 2\int_{\frac{2\pi}{3}}^{\frac{2\pi}{3}+\Lambda} \frac{dk'}{2\pi} \frac{-\frac{3}{4}\left(1-\frac{3\Delta^2}{v^2}\right)Q^2}{v\left(2k+Q-\frac{4\pi}{3}\right)-\sqrt{3}\Delta Q} \sum_{l'=0}^{\infty} U\Phi_{l'}(0).\end{aligned} \tag{A4}$$

In the second and the third lines we have approximated $\Phi_{l'}(Q) \approx \Phi_{l'}(0)$, assuming that $\Phi_l(Q)$ is well behaved at $Q = 0$ and any difference is $O(Q)$. In the third line we have retained the most singular contribution at $O(Q^2)$, which is in the vicinity of the Dirac points (hence the factor of 2), as the remaining terms contain no infrared divergence.

Using Eq. (A2) and recalling that the $Q = 0$ solution is $f(k;0) = 1$, we have

$$\sum_{l'=0}^{\infty} U\Phi_{l'}(0) = \sum_{l'=0}^{\infty} \int_{\frac{2\pi}{3}}^{\frac{4\pi}{3}} \frac{dk}{2\pi} g_0^2(k) U \left(4\cos^2\frac{k}{2}\right)^{l'} = \frac{U}{3} \tag{A5}$$

and

$$\sum_{l'=0}^{\infty} \left(4\cos^2\frac{k'}{2}\right)^{l'} U\Phi_{l'}(0) = \sum_{l'=0}^{\infty} \int_{\frac{2\pi}{3}}^{\frac{4\pi}{3}} \frac{dk}{2\pi} g_0^2(k) U \left(16\cos^2\frac{k}{2}\cos^2\frac{k'}{2}\right)^{l'} = \frac{\epsilon_h(k') + \epsilon_p(k')}{1 - 4\cos^2\frac{k'}{2}}; \tag{A6}$$

therefore

$$\begin{aligned}\Phi_l(Q) = {} & \int \frac{dk'}{2\pi} \frac{\left(1 - 4\cos^2\frac{k'}{2}\right)^2}{\epsilon_h(k') + \epsilon_p(k')} \left(4\cos^2\frac{k'}{2}\right)^l \sum_{l'=0}^{\infty} \left(4\cos^2\frac{k'}{2}\right)^{l'} U\Phi_{l'}(Q) \\ & + E \int \frac{dk'}{2\pi} \frac{1 - 4\cos^2\frac{k'}{2}}{\epsilon_h(k') + \epsilon_p(k')} \left(4\cos^2\frac{k'}{2}\right)^l - \frac{1}{8\pi v}\left(1 - \frac{3\Delta^2}{v^2}\right) Q^2 U \ln\frac{\Lambda'}{Q}.\end{aligned} \tag{A7}$$

Now, we multiply the entire expression by $[1 - 4\cos^2(k/2)][4\cos^2(k/2)]^l U$, then sum over l and integrate over k. The left-hand side then cancels the first term on the right-hand side, and using $v = U/(2\sqrt{3})$, we are left with Eq. (35).

In the presence of nonlocal interactions, one needs to assign three more indices to Φ, namely δ_m, δ_n, and $\alpha = 1, 2$ [corresponding to the two terms in the third line of Eq. (23)]. All three indices should be summed over in Eq. (A3) and, subsequently, in Eqs. (A5), (A6), and (A7).

[1] M. Fujita, K. Wakabayashi, K. Nakada, and K. Kusakabe, J. Phys. Soc. Jpn. **65**, 1920 (1996).
[2] K. Wakabayashi, K.-i. Sasaki, T. Nakanishi, and T. Enoki, Sci. Technol. Adv. Mater. **11**, 054504 (2010).
[3] O. V. Yazyev, Rep. Prog. Phys. **73**, 056501 (2010).
[4] A. Yamashiro, Y. Shimoi, K. Harigaya, and K. Wakabayashi, Phys. Rev. B **68**, 193410 (2003).
[5] J. Jung, T. Pereg-Barnea, and A. H. MacDonald, Phys. Rev. Lett. **102**, 227205 (2009); J. Jung and A. H. MacDonald, Phys. Rev. B **79**, 235433 (2009).
[6] J.-W. Rhim and K. Moon, Phys. Rev. B **80**, 155441 (2009).
[7] M. J. Schmidt and D. Loss, Phys. Rev. B **82**, 085422 (2010).
[8] J. Jung, Phys. Rev. B **83**, 165415 (2011).
[9] F. J. Culchac, A. Latgé, and A. T. Costa, New J. Phys. **13**, 033028 (2011).
[10] M. J. Schmidt, Phys. Rev. B **86**, 075458 (2012).
[11] H. Karimi and I. Affleck, Phys. Rev. B **86**, 115446 (2012).
[12] D. J. Luitz, F. F. Assaad, and M. J. Schmidt, Phys. Rev. B **83**, 195432 (2011); M. J. Schmidt, M. Golor, T. C. Lang, and S. Wessel, *ibid.* **87**, 245431 (2013).
[13] B. Wunsch, T. Stauber, F. Sols, and F. Guinea, Phys. Rev. Lett. **101**, 036803 (2008).
[14] M. Golor, T. C. Lang, and S. Wessel, Phys. Rev. B **87**, 155441 (2013).
[15] M. Golor, C. Koop, T. C. Lang, S. Wessel, and M. J. Schmidt, Phys. Rev. Lett. **111**, 085504 (2013).
[16] M. Golor, S. Wessel, and M. J. Schmidt, Phys. Rev. Lett. **112**, 046601 (2014).
[17] I. Hagymási and O. Legeza, Phys. Rev. B **94**, 165147 (2016).
[18] Y.-W. Son, M. L. Cohen, and S. G. Louie, Phys. Rev. Lett. **97**, 216803 (2006).
[19] L. Pisani, J. A. Chan, B. Montanari, and N. M. Harrison, Phys. Rev. B **75**, 064418 (2007).
[20] L. F. Huang, G. R. Zhang, X. H. Zheng, P. L. Gong, T. F. Cao, and Z. Zeng, J. Phys. Condens. Matter **25**, 055304 (2013).
[21] K. Wakabayashi, M. Sigrist, and M. Fujita, J. Phys. Soc. Jpn. **67**, 2089 (1998).
[22] O. V. Yazyev and M. I. Katsnelson, Phys. Rev. Lett. **100**, 047209 (2008).
[23] Y.-T. Zhang, H. Jiang, Q.-f. Sun, and X. C. Xie, Phys. Rev. B **81**, 165404 (2010).
[24] G. Z. Magda, X. Jin, I. Hagymási, P. Vancsó, Z. Osváth, P. Nemes-Incze, C. Hwang, L. P. Biró, and L. Tapasztó, Nature (London) **514**, 608 (2014).
[25] P. Ruffieux, S. Wang, B. Yang, C. Sánchez-Sánchez, J. Liu, T. Dienel, L. Talirz, P. Shinde, C. A. Pignedoli, D. Passerone, T. Dumslaff, X. Feng, K. Müllen, and R. Fasel, Nature (London) **531**, 489 (2015).
[26] T. L. Makarova, A. L. Shelankov, A. A. Zyrianova, A. I. Veinger, T. V. Tisnek, E. Lähderanta, A. I. Shames, A. V. Okotrub, L. G. Bulusheva, G. N. Chekhova, D. V. Pinakov, I. P. Asanov, and Ž. Šljivančanin, Sci. Rep. **5**, 13382 (2015).
[27] E. H. Lieb, Phys. Rev. Lett. **62**, 1201 (1989).
[28] D. P. DiVincenzo and E. J. Mele, Phys. Rev. B **29**, 1685 (1984).
[29] V. N. Kotov, B. Uchoa, V. M. Pereira, F. Guinea, and A. H. Castro Neto, Rev. Mod. Phys. **84**, 1067 (2012).
[30] W. Wu and A.-M. S. Tremblay, Phys. Rev. B **89**, 205128 (2014).
[31] I. F. Herbut, Phys. Rev. Lett. **97**, 146401 (2006).
[32] C. Honerkamp, Phys. Rev. Lett. **100**, 146404 (2008).

[33] M. Schüler, M. Rösner, T. O. Wehling, A. I. Lichtenstein, and M. I. Katsnelson, Phys. Rev. Lett. **111**, 036601 (2013).
[34] S. Chacko, D. Nafday, D. G. Kanhere, and T. Saha-Dasgupta, Phys. Rev. B **90**, 155433 (2014).
[35] L. Y. Zhu and W. Z. Wang, J. Phys. Condens. Matter **18**, 6273 (2006).
[36] N. D. Mermin and H. Wagner, Phys. Rev. Lett. **17**, 1133 (1966).
[37] R. Egger and A. O. Gogolin, Phys. Rev. Lett. **79**, 5082 (1997).
[38] M. Zarea and N. Sandler, Phys. Rev. Lett. **99**, 256804 (2007); M. Zarea, C. Büsser, and N. Sandler, *ibid.* **101**, 196804 (2008).
[39] V. M. Pereira, F. Guinea, J. M. B. Lopes dos Santos, N. M. R. Peres, and A. H. Castro Neto, Phys. Rev. Lett. **96**, 036801 (2006).
[40] J. González, F. Guinea, and M. A. H. Vozmediano, Phys. Rev. B **59**, R2474 (1999).
[41] J. Jiang, R. Saito, G. G. Samsonidze, A. Jorio, S. G. Chou, G. Dresselhaus, and M. S. Dresselhaus, Phys. Rev. B **75**, 035407 (2007); R. M. Konik, Phys. Rev. Lett. **106**, 136805 (2011); S. Konabe, K. Matsuda, and S. Okada, *ibid.* **109**, 187403 (2012).
[42] M. Abramowitz and I. Stegun, *Handbook of Mathematical Functions: With Formulas, Graphs, and Mathematical Tables*, Dover Books on Mathematics (Dover Publications, New York, 2012).
[43] C. Koop and M. J. Schmidt, Phys. Rev. B **92**, 125416 (2015).
[44] L. Brey and H. A. Fertig, Phys. Rev. B **73**, 235411 (2006).